Kinetic mechanism of octopus hepatopancreatic glutathione transferase in reverse micelles

Shiao-Shek TANG and Gu-Gang CHANG*

Graduate Institutes of Life Sciences and Biochemistry, National Defence Medical Centre, Taipei, Taiwan, Republic of China

Octopus glutathione transferase (GST) was enzymically active in aerosol-OT [sodium bis-(2-ethylhexyl)sulphosuccinate]/iso-octane reverse micelles albeit with lowered catalytic constant (k_{cat}). The enzyme reaction rate was found to be dependent on the [H_2O]/[surfactant] ratio (ω_o) of the system with maximum rate observed at ω_o 13.88, which corresponded to vesicles with a core volume of 64 nm^3. According to the physical examinations, a vesicle of this size is barely large enough to accommodate a monomeric enzyme subunit. Dissociation of the enzyme in reverse micelles was confirmed by cross-linking of the associated subunits with glutaraldehyde and separation of the monomers and dimers with electrophoresis in the presence of SDS. The kinetic properties of the enzyme were investigated by steady-state kinetic analysis. Both GSH and 1-chloro-2,4-dinitrobenzene (CDNB) showed substrate inhibition and the Michaelis constant for CDNB was increased by 36-fold to 11.05 mM in reverse micelles. Results on the initial-velocity and product-inhibition studies indicate that the octopus GST conforms to a steady-state sequential random Bi Bi mechanism. The results from a log k_{cat} versus pH plot suggest that amino acid residues with pK_a values of 6.56 ± 0.07 and 8.81 ± 0.17 should be deprotonated to give optimum catalytic function. In contrast, the amino acid residue with a pK_a value of 9.69 ± 0.16 in aqueous solution had to be protonated for the reaction to proceed. We propose that the pK_{a1} (6.56) is that for the enzyme-bound GSH, which has a pK_a value lowered by 1.40–1.54 pH units compared with that of free GSH in reverse micelles. The most probable candidate for the observed pK_{a2} (8.81) is Tyr^7 of GST. The pK_a of Tyr^7 is 0.88 pH unit lower than that in aqueous solution and is about 2 pH units below the normal tyrosine. This tyrosyl residue may act as a base catalyst facilitating the dissociation of enzyme-bound GSH. The possible interaction of GST with plasma membrane *in vivo* is discussed.

INTRODUCTION

Glutathione transferase (GST; EC 2.5.1.18) is a cytosolic detoxication enzyme [1–4]. It catalyses the conjugation of glutathione with a broad range of xenobiotic hydrophobic compounds resulting in a more water-soluble product being eliminated from the cell by a glutathione conjugate-pump system in the plasma membrane [5]. We have isolated the enzyme from octopus hepatopancreas to apparent homogeneity [6]. The kinetic properties of the enzyme in aqueous solution were studied by a steady-state approach [7]. In that study the water-insoluble substrate was added as a DMSO solution. Considering the conjugation reaction *in vivo*, the exogenous hydrophobic compounds preferred to be in the cell membranous lipid bilayer structure. There is always a partition between the aqueous and the hydrocarbon phases.

To mimic the *in vivo* conditions, we entrapped the octopus GST in several reverse micellar systems. Reverse micelles are water droplets, 1–10 nm in diameter, dispersed in organic solvent by means of a surfactant which forms a transparent macrohomogeneous solution and can be examined with various optical instruments [8–13]. Enzymes in reverse micelles can convert polar and apolar substrates [14]. It is an ideal system in which to study the enzymic reactions with water-insoluble substrates. In this paper, we report the steady-state kinetics of the enzyme in several reverse micellar systems. The kinetic data thus obtained were compared with those in the aqueous medium [7]. To our knowledge, this is the first report on the enzymic activity of GST in reverse micelles. Its implications on the *in vivo* conditions are discussed.

MATERIALS AND METHODS

Materials

Aerosol-OT {AOT; [sodium bis-(2-ethylhexyl)sulphosuccinate]}, CTAB (cetyltrimethylammonium bromide), CDNB (1-chloro-2,4-dinitrobenzene), GSH and Triton X-100 were purchased from Sigma (St. Louis, MO, U.S.A.). Iso-octane (2,2,4-trimethylpentane) and n-hexanol were purchased from E. Merck (Darmstadt, Germany). *S*-(2,4-Dinitrophenyl)glutathione [S-(DNP)GS] was synthesized non-enzymically from GSH and CDNB as described previously [15]. Other chemicals used were as described previously [6,7].

Stock reverse micellar solutions were prepared as described previously [16]. The average inclusive radius (R_c) of the AOT/iso-octane reverse micellar vesicles was estimated by the following empirical formula (eqn. 1) [17].

$$R_c\ (\text{nm}) = 0.15\ \omega_o + 0.4 \quad (1)$$

where ω_o is the hydration degree ([H_2O]/[AOT]) of the system in terms of molar concentration for both components.

Abbreviations used: AOT, aerosol OT [sodium bis-(2-ethylhexyl)sulphosuccinate]; CDNB, 1-chloro-2,4-dinitrobenzene; CTAB, cetyltrimethylammonium bromide; GST, glutathione S-transferase; S-(DNP)GS, *S*-(2,4-dinitrophenyl)glutathione; ω_o, the ratio of water concentration and AOT concentration ([H_2O]/[AOT]).

* To whom correspondence should be addressed.

The partition of CDNB between aqueous and organic phases in various reverse micellar systems was determined according to the procedure of Tyrakowska et al. [18].

Enzyme purification

Octopus digestive gland GST was purified by a single GSH-Sepharose 4B affinity chromatography step as described in the literature [6]. The dimeric enzyme was judged to be apparently homogeneous by SDS/PAGE with subunit M_r 24000. Protein concentration was determined by the protein-dye binding method [19].

Determination of octopus GST activity

The activity of octopus GST in aqueous solution was assayed at 25 °C according to our previously described procedure [6,7].

In reverse micellar systems, the water pool consisted of Bistris buffer (200 mM, pH 6.5). To 2.5 ml of stock reverse micellar solution (already containing the desired CDNB concentration), iso-octane and aliquots of GSH and enzyme solution were added to give a final volume of 3 ml and $[H_2O]$/[surfactant] ratio of 13.88 [water content of the system 5 % (v/v), given as a percentage of the total volume]. Under these conditions the micellar concentration was estimated to be 7.8 mM, and the numbers of surfactant molecules/micelle were estimated, according to a second-order polynomial equation [20], to be 183. A theoretical treatment considering the number of substrate molecules per reverse micelle was given by Verhaert et al. [21]. The conjugation reaction was followed by continuous monitoring of the change in absorbance at 340 nm using a Perkin-Elmer Lambda 3B spectrophotometer with appropriate correction for the minor non-enzymic conjugation as described by Chang et al. [15]. A molar absorption coefficient of $9.6 \times 10^3\ M^{-1} \cdot cm^{-1}$ for the conjugate was used in the calculation [22]. All concentration calculations were based on the final total volume and not the small water pool entrapped in reverse micelles [8,23].

We found that the absorption coefficients of S-(DNP)GS in aqueous, AOT/iso-octane/water, CTAB/iso-octane/n-hexanol/water, or Triton X-100/iso-octane/n-hexanol/water reverse micellar systems were identical. In all assay systems, the reaction rate was found to be linear with time for at least 3 min under the experimental conditions. The dependence of reaction rate on enzyme concentration was also linear up to 3.69 μg/assay. After completion of the assay, the conjugated substrate only accounts for less than 1.6 % of the original substrate concentration.

Chemical cross-linking and SDS/PAGE

Chemical cross-linking of the associated dimers of GST and separation of dimers and monomers were performed according to our published procedure with some modifications [6,24,25]. To minimize the interference of AOT in PAGE, GST (16.11 μg) was cross-linked with glutaraldehyde (6.25 mM) in Tris/HCl buffer (50 mM, pH 7.7) in reverse micelles with various ω_o values. The total volume was 1 ml. After cross-linking at room temperature (25 °C) for 20 min, 30 μl of Tris/HCl buffer (0.5 M, pH 8.5) was added and the solution was stored at −20 °C overnight to allow the aqueous phase to freeze. After removing the upper iso-octane phase, the lower aqueous phase was centrifuged at 5000 ***g*** for 5 min, which separated the system into two phases. Aliquot samples from the bottom phase were withdrawn to perform the SDS/PAGE as described previously [6,25].

The protein recovery of the above procedure is influenced by the AOT concentration. At large [AOT] (i.e. small ω_o), the protein band is very faint, which makes the quantification difficult; however, the relative amounts of dimers and monomers are easily estimated.

Initial-velocity and product-inhibition studies

Initial-velocity studies were performed by varying the concentrations of GSH from 0.1 to 0.7 mM and CDNB from 0.5 to 6 mM. Concentrations of other components were held constant.

Inhibition studies were performed in a similar manner as described for initial-velocity studies with S-(DNP)GS as product inhibitor. The inhibitor was held at several fixed concentrations close to its inhibition constant (K_i).

pH studies

We assayed the enzyme activity at various pH values with two substrate concentrations at 25 °C. The experimental conditions in aqueous solution were as described [7]. In reverse micelles when the enzyme was assayed at high substrate concentration, the CDNB and GSH concentrations were 7 mM and 1 mM respectively. The velocities thus obtained were near maximum velocity (V_{max}). Enzyme activity was calculated according to the Michaelis–Menten equation [eqn. (2)] to give the apparent first-order rate constant (k_{cat}).

$$v = V_{max}[S]/(K_m + [S]) \quad (2)$$

where [S] denotes substrate concentration and K_m is the Michaelis constant. k_{cat} was obtained by dividing V_{max} by $[E_t]$, the total concentration of enzyme.

When the enzyme was assayed at a low CDNB concentration, the GSH concentration was fixed at 1 mM, which was approximately 4-fold its K_m and the CDNB concentration employed was 1 mM, about 0.09 times its K_m. The initial rates were then approximately equal to $V_{max}[S]/K_m$. The second-order rate constant ($k_{cat}/K_{m,CDNB}$) was obtained by dividing v by $[CDNB][E_t]$. Experiments with saturated CDNB were not feasible because of strong substrate inhibition.

The pH value of reverse micellar solution was determined by directly immersing the glass electrode into the transparent reverse micellar solution. pH values of the reverse micellar solutions were the same as those in aqueous solution, which indicates that the pH of the water pool is close to that of the initial buffer system, in accordance with the generally accepted conception about the pH of a reverse micellar system at $[H_2O]$/[surfactant] > 10–15 [13,26].

Data processing

For wide range substrate concentrations, the rate versus [S] data were fitted to eqn. (3) to calculate the substrate inhibition constant (K_{iS}) and K_m.

$$v = V_{max}[S]/(K_m + [S] + [S]^2/K_{iS}) \quad (3)$$

Data conforming to a linear non-competitive inhibition pattern or to a sequential initial-velocity pattern were fitted to eqns. (4) and (5) respectively.

$$v = V_{max}/\{(1 + K_m/[S]) \cdot (1 + [I]/K_i)\} \quad (4)$$

$$v = V_{max}[GSH][CDNB]/(K_{d,GSH}K_{m,CDNB} + K_{m,GSH}[CDNB] + K_{m,CDNB}[GSH] + [GSH][CDNB]) \quad (5)$$

where [I] is the inhibitor concentration, K_i denotes the inhibition constant, $K_{m,GSH}$ and $K_{m,CDNB}$ are Michaelis constants for GSH and CDNB respectively, and $K_{d,GSH}$ is the dissociation constant for GSH. We used the EZ-FIT computer program [27] or a

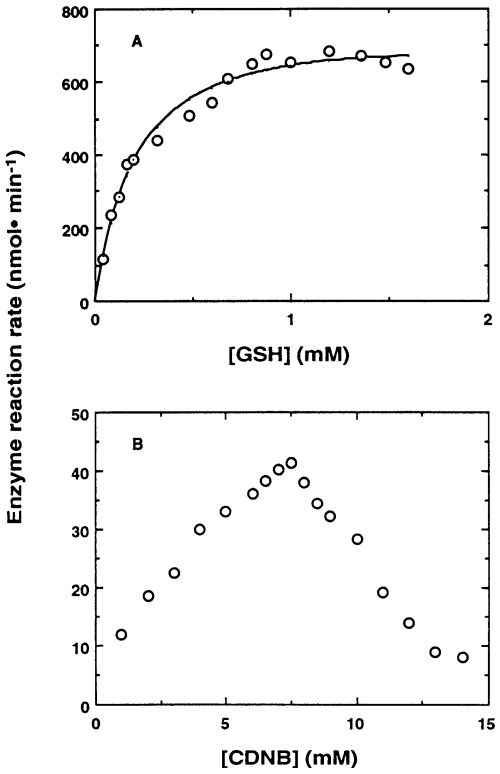

Figure 1 Effect of substrate concentration on the GST-catalysed reaction in AOT/iso-octane/water reverse micelles

(**A**) Effect of [GSH] on the reaction rate. (**B**) Effect of [CDNB] on the reaction rate. The points are experimental data and the curve is computer fitted to eqn. (3). The GST amount used was 0.64 μg/assay. The [H_2O]/[AOT] ratio was fixed at 13.88.

generally applicable non-linear-regression program SigmaPlot (Jandel Scientific, San Raefel, CA, U.S.A.) in fitting our data for calculating the various kinetic parameters.

For pH studies, when the pH versus rate profiles were decreased at both low and high pH values, the data were fitted to eqn. (6). For those profiles that were decreased only at low pH, fitting to eqn. (7) was applied.

$$\log\ Y = \log\ \{C/(1+[H^+]/K_{a1}+K_{a2}/[H^+])\} \quad (6)$$

$$\log\ Y = \log\ \{C/(1+[H^+]/K_{a1})\} \quad (7)$$

where Y is the parameter measured at various pH values, C is the pH-independent value of Y, and K_{a1} and K_{a2} are dissociation constants for the enzyme groups.

A profile that decreased at low pH but increased at high pH values with two optima describes a complex mechanism involving two catalytically active species E^nS and $E^{n-1}S$ with V_{max} and V_{max}' respectively; where $V_{max}' = \gamma V_{max}$ and $\gamma > 1$ [28,29]. The data were fitted to an equation we derived recently [eqn. (8)] [28]:

$$\log\ Y = \log\ \{C(1+\gamma K_{a2}/[H^+])/(1+[H^+]/K_{a1}+K_{a2}/[H^+])\} \quad (8)$$

RESULTS

Effect of substrate concentration on the enzyme reaction rate

In aqueous solution, when the enzyme assays were conducted with various concentrations of GSH or CDNB, the enzyme was observed to be saturated at a concentration of 1.36 mM for GSH and 1.5 mM for CDNB. No substrate inhibition was observed for GSH up to 3.6 mM or for CDNB up to 3 mM. The apparent $K_{m,GSH(app.)}$ and $K_{m,CDNB(app.)}$ values were estimated to be 0.16 ± 0.03 mM and 0.39 ± 0.07 mM respectively.

The octopus GST was found to be enzymically active when embedded in AOT/iso-octane reverse micelles; however, varying kinetic behaviour was observed (Figure 1). At GSH concentrations above 1 mM and CDNB concentrations above 7 mM, substrate inhibition was observed. The apparent $K_{m,GSH(app.)}$ (0.46 ± 0.12 mM) was similar to that in the aqueous solution. The $K_{m,CDNB(app.)}$ (9.44 ± 0.87 mM), on the other hand, was greatly increased in reverse micelles. Fitting of the initial rate to eqn. (3) obtained K_{iS} for GSH ($K_{i,GSH}$) of 2.8 ± 1.3 mM. The data on CDNB could not be fitted to eqn. (3).

The octopus GST was also active in CTAB/iso-octane/n-hexanol or Triton X-100/iso-octane/n-hexanol reverse micellar systems. The apparent kinetic parameters of the enzyme in those systems are summarized in Table 1.

GST assay in the AOT/iso-octane system has advantages. No co-surfactant (e.g. n-hexanol) is necessary. Furthermore, the non-enzymic conjugation between GSH and CDNB decreased in this system [16]. Background correction was minimal. For these reasons, detailed kinetic studies of GST in reverse micelles were examined with an AOT/iso-octane system.

Effect of [H_2O]/[AOT] (ω_o) on the enzyme-catalysed reaction

The catalytic activity of GST in reverse micelles was assayed at various ω_o values, which were prepared by varying the H_2O concentrations and keeping the AOT concentration constant or

Table 1 Apparent kinetic constants for octopus hepatopancreatic GST in various reverse micellar or aqueous systems

All values shown are averages $\pm$ S.E.M. ($n = 15$). The [H_2O]/[surfactant] ratio was maintained constant at 13.88.

Solvent systems	Partition coefficient of CDNB	$K_{m,GSH(app.)}$ (mM)	$K_{i,GSH(app.)}$ (mM)	$K_{m,CDNB(app.)}$ (mM)	$K_{m,CDNB(app.)}'$ (mM)[a]	$V_{max,GSH(app.)}$ (μmol/min)	$V_{max,CDNB(app.)}$ (μmol/min)
Aqueous	–	0.16 ± 0.03	–	0.39 ± 0.07	–	0.83 ± 0.06	0.97 ± 0.07
Reverse micelles							
AOT	12.34	0.46 ± 0.12	2.8 ± 1.3	9.44 ± 0.87	0.76 ± 0.07	0.17 ± 0.05	0.19 ± 0.01
CTAB	14.74	0.40 ± 0.11	–[b]	3.90 ± 1.10	0.26 ± 0.01	0.47 ± 0.06	0.23 ± 0.04
Triton X-100	13.64	0.24 ± 0.04	–[b]	4.36 ± 0.91	0.32 ± 0.07	0.20 ± 0.01	0.15 ± 0.02

[a] Calculated from $K_{m,CDNB}$ by taking into account the partition coefficient of CDNB.
[b] Not determined.

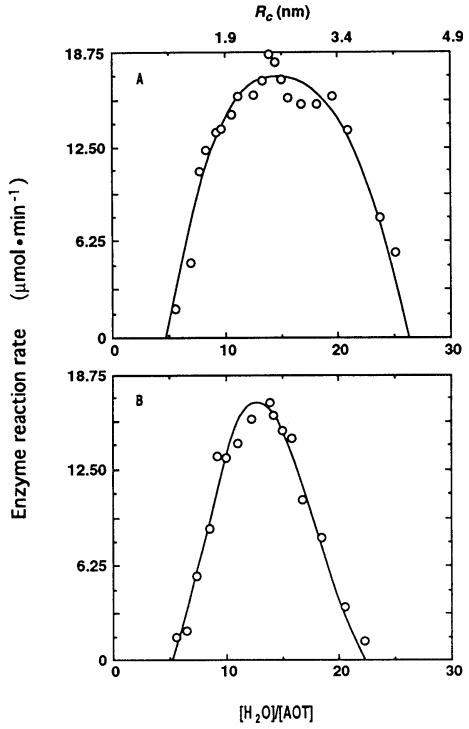

Figure 2 Effect of $[H_2O]/[AOT]$ ratio (ω_o) of a reverse micellar system on the rate of reaction catalysed by octopus GST

The enzyme activities were assayed at different ω_o values by maintaining the water concentration constant and varying the AOT concentration (**A**), or by keeping the AOT concentration constant but varying the water concentration (**B**). The GST amount used was 0.64 μg/assay. The inclusive radii of the reverse micellar vesicles were estimated by eqn. (1) and is shown on the top scale.

vice versa. Both systems gave a rate versus ω_o profile with a maximum activity observed at ω_o 13.88 (Figure 2). Reverse micelles with this hydration degree were estimated to have an inclusion radius of 2.48 nm and an inclusion volume of 64 nm^3 [17].

Dissociation of octopus hepatopancreatic GST in reverse micelles

Considering that the dimeric GST will occupy a volume of approximately 145 nm^3 [30–34], the above results suggest that octopus GST could be dissociated in AOT/iso-octane reverse micelles. To confirm this possibility we cross-linked the enzyme in reverse micelles with glutaraldehyde, and separated the monomers and dimers with SDS/PAGE. The data presented in Figure 3 clearly indicate that most of the dimeric enzyme dissociated into monomers. At ω_o 13.88, approximately 85% of the enzyme had dissociated into monomers. No dimer is detectable at ω_o 10.4. Extrapolating the line shown in Figure 3(B) to 100% dimer corresponded to a theoretical ω_o value of 55, where no dissociation occurred. This ω_o value approached the molarity of pure water (55.5 M).

Effect of AOT concentration on the GST-catalysed reaction rate in reverse micelles

The effect of detergent on the enzyme reaction rate was examined by assaying the enzyme activity in AOT/iso-octane reverse micelles by increasing both AOT and H_2O concentrations. The $[H_2O]/[AOT]$ ratio of the system was kept constant, which will

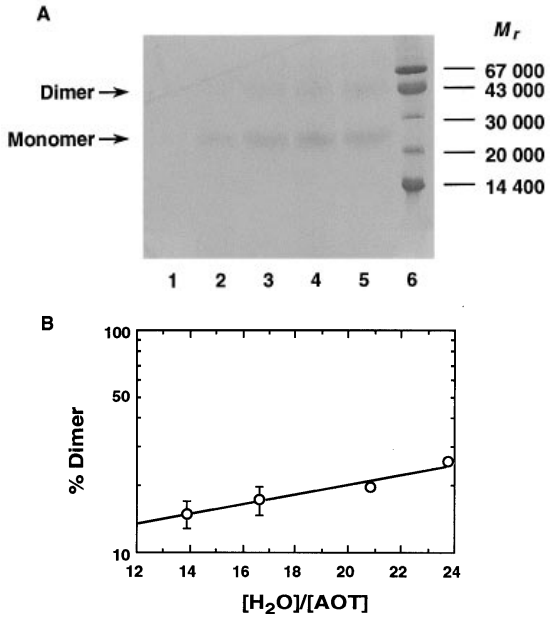

Figure 3 Dissociation of octopus hepatopancreatic GST in reverse micelles

(**A**) SDS/PAGE of the chemically cross-linked GST was performed with 20% homogeneous PhastGel for 113 V · h. For lanes 1–5, the $[H_2O]/[AOT]$ is 10.4, 13.88, 16.65, 20.83, and 23.78 respectively. Lane 6 is the M_r markers. The protein amounts applied were 16.11 μg in each lane. (**B**) Logarithmic relationship between the $[H_2O]/[AOT]$ ratio and the percentage of undissociated dimer.

maintain a constant inclusive volume for the reverse micelles but increase the micelle concentration [11]. The detergent concentration is thus increased. Since the reverse micellar system is in dynamic equilibrium, colliding with each other on a 10^{-10} s time scale [13], and the solubilized components exchange with a second-order rate constant of 10^6–10^8 $dm^3 \cdot mol^{-1} \cdot s^{-1}$ [35], the entrapped GST molecules will experience higher surfactant concentrations as the AOT concentration increases, because the probability of GST encountering empty micelle particles will increase as the number of reverse micellar vesicles increases. The

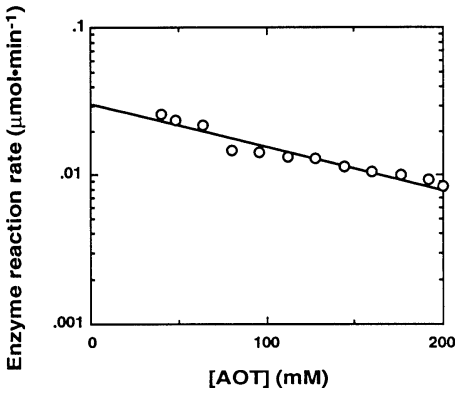

Figure 4 Effect of AOT concentration on the GST-catalysed reaction rate in reverse micelles

The increase of [AOT] was achieved by increasing the [AOT] and $[H_2O]$ simultaneously. The dimensions of the reverse micelles remained the same by keeping the $[H_2O]/[AOT]$ ratio constant at 13.88. GST amount used was 0.83 μg/assay.

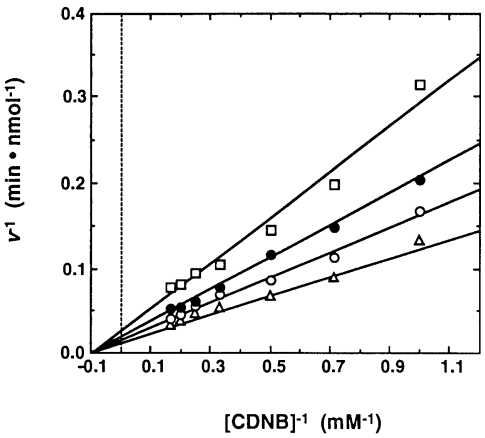

Figure 5 Initial-velocity pattern for octopus hepatopancreatic GST in AOT/iso-octane reverse micelles

The varied-concentration substrate was CDNB and the fixed-concentration substrate was GSH. The concentration of GSH was 0.1 (□), 0.2 (●), 0.4 (○), and 0.7 mM (△). The points are experimental data and lines are computer fitted to eqn. (5). GST amount used was 0.64 μg/assay.

chance of GST molecules coming into contact with the AOT molecule will increase in this case.

Octopus GST was found to be sensitive to the AOT concentration. The enzyme activity decreased exponentially as the AOT concentration increased (Figure 4).

Initial-velocity studies

The initial-velocity pattern of GST-catalysed conjugation between non-inhibitory concentrations of GSH and CDNB in AOT/iso-octane reverse micellar media is shown in Figure 5. When CDNB was plotted as the varied-concentration substrate with different concentrations of GSH as the fixed-concentration substrate, an intersecting pattern was obtained. This result excludes a Ping Pong kinetic mechanism but conforms to a sequential mechanism. Since a linear $1/v$ versus $1/[S]$ plot was obtained, the data were fitted to eqn. (5) to calculate the various kinetic parameters, which are shown in Table 2.

A similar intersecting pattern was obtained in aqueous solution [7]. The kinetic parameters were also summarized in Table 2 for comparison. The catalytic constant (k_{cat}) for the enzyme in reverse micelles decreased by 0.63-fold compared with that in aqueous solution. The K_m values for GSH and CDNB were increased 2.3- and 36-fold respectively. Binding of one substrate seems to interfere with the binding of the other substrate. The K_d values were smaller than the K_m values (Table 2).

To distinguish the random versus ordered sequential mechanism, product-inhibition studies are required.

Product-inhibition studies

Product-inhibition patterns were analysed to examine the detailed kinetic mechanism of GST in AOT/iso-octane reverse micelles. With S-(DNP)GS as the inhibitor and either GSH or CDNB as the varied-concentration substrate, a linear non-competitive inhibition pattern was obtained (Figure 6). An inhibition pattern by the other product, Cl^-, was not feasible because the K_i is very large ($\sim$500 mM), a concentration which is insoluble in the reverse micellar solution.

The above results are enough to deduce a steady-state random Bi Bi kinetic mechanism for the octopus GST in AOT/iso-octane reverse micelles, because a rapid equilibrium random Bi Bi mechanism would result in competitive inhibition patterns for all products [29]. The inhibition constants for the conjugate [$K_{i,S\text{-}(DNP)GS}$] obtained by fitting the data to eqn. (4) are listed in Table 2.

pH studies

The purified octopus GST is stable under the assay conditions between pH 5.5 and pH 10.0 for at least 20 min in aqueous and

Table 2 Comparison of kinetic parameters of octopus hepatopancreatic GST in AOT/iso-octane reverse micellar and aqueous systems

All values shown are averages $\pm$ S.E.M. ($n = 28$ in initial-velocity experiment and $n = 15$ or 10 in pH studies).

Kinetic constant	Description	Value	
		Aqueous	Reverse micelles
k_{cat}	Catalytic constant	213 ± 8.1 s^{-1}*	135 ± 30 s^{-1}
$K_{m,GSH}$	Dissociation constant of CDNB–E–GSH to give E–CDNB and GSH	0.149 ± 0.017 mM*	0.291 ± 0.125 mM
$K_{m,CDNB}$	Dissociation constant of CDNB–E–GSH to give E–GSH and CDNB	0.333 ± 0.030 mM*	11.05 ± 3.34 mM
$K_{d,GSH}$	Dissociation constant of E–GSH to give GST and GSH	0.344 ± 0.004 mM*	0.130 ± 0.04 mM
$K_{d,CDNB}$	Dissociation constant of E–CDNB to give GST and CDNB	0.769 ± 0.007 mM*	4.936 ± 0.988 mM
$K_{i,S\text{-}(DNP)GS}$	Dissociation constant of CDNB–E–S-(DNP)GS to give E–CDNB and S-(DNP)GS	39.6 ± 2.42 μM*	375.2 ± 38.9 μM
$K_{i,S\text{-}(DNP)GS}'$	Dissociation constant of GSH–E–S-(DNP)GS to give E–GSH and S-(DNP)GS	53.7 ± 3.93 μM*	970.7 ± 140.4 μM
pK_{es}	Molecular pK_a value in the CDNB–E–GSH complex	6.70 ± 0.09 9.69 ± 0.16	6.56 ± 0.07 8.81 ± 0.17
pK_e	Molecular pK_a value in the E–GSH complex	6.80 ± 0.40 10.11 ± 0.11	6.70 ± 0.05

* From Tang and Chang [7].

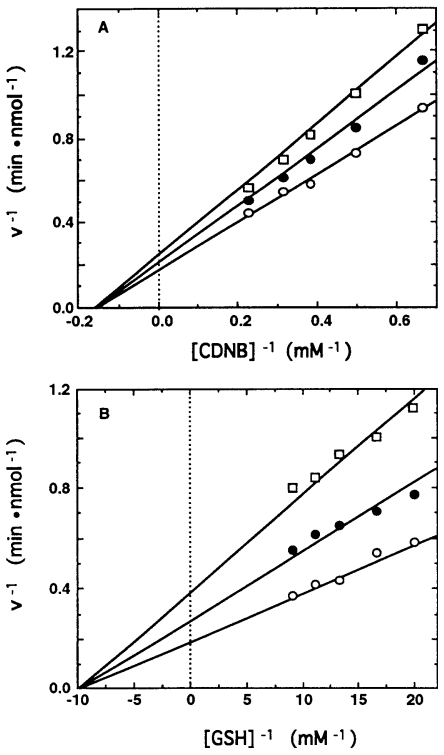

Figure 6 Product-inhibition patterns of octopus hepatopancreatic GST by S-(DNP)GS in AOT/iso-octane reverse micelles

Non-competitive inhibition of the conjugation reaction by S-(DNP)GS with respect to CDNB (**A**) or GSH (**B**). The S-(DNP)GS concentration was 0 (○), 212.5 μM (●), and 318.7 μM (□) respectively, in (**A**); and 0 (○), 213.3 μM (●), and 243.6 μM (□) respectively, in (**B**). The points are experimental data and lines are computer fitted to eqn. (4). GST amount used was 0.64 μg/assay.

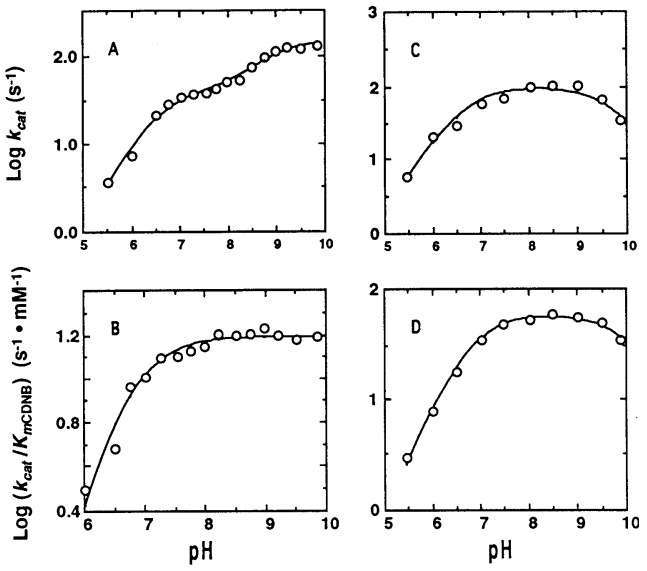

Figure 7 Effect of pH on the octopus hepatopancreatic GST catalysed reaction in reverse micelles

The effects of pH on k_{cat} (**A**, **C**) or k_{cat}/K_m (**B**, **D**) were determined at various pH values with Bis-tris-propane buffer (200 mM). (**A** and **B**) Reverse micellar solution with [H_2O]/[AOT] at 13.88. (**C** and **D**) Aqueous solution. The points represent the experimental data and the lines denote the computer fit using eqn. (8) in (**A**) , eqn. (6) in (**B**), and eqn. (7) in (**C**) and (**D**). GST amount used was 0.64 μg/assay.

reverse micelles. Detailed pH effects on the enzyme activity were studied over this pH range. Substantially different results were obtained with the aqueous or reverse micellar systems. The important observations are illustrated in Figure 7. In aqueous solution, the plot of k_{cat} versus pH produced a bell-shaped curve. Fitting the data to eqn. (6) allowed us to estimate two pK_a values of 6.70 ± 0.09 and 9.69 ± 0.16 for the ES complex (Figure 7C), which indicated that during the catalysis an amino acid residue with a pK_a value of 6.70 must be deprotonated and another residue with a pK_a value of 9.69 must be protonated to obtain maximum activity for the enzyme.

From the log ($k_{cat}/K_{m,CDNB}$) versus pH plot (Figure 7D), two molecular pK_a values of 6.80 ± 0.40 and 10.11 ± 0.11 were detected for the E–GSH binary complex in aqueous solution. The former and the latter had to be deprotonated and protonated, respectively, for the reaction to proceed.

In reverse micelles, entirely different results were obtained. Two pK_a values of 6.56 ± 0.07 and 8.81 ± 0.17 were detected from the log k_{cat} versus pH plot (Figure 7A). These pK_a values were smaller than those found in the aqueous solution. However, in contrast to aqueous solution, the amino acid residue with pK_a value of 8.81 was deprotonated to give another activity plateau. These experiments were repeated several times and the same results were obtained. Only one molecular pK_a of 6.70 ± 0.05, which had to be deprotonated, was detected in the E–GSH binary complex from the log ($k_{cat}/K_{m,CDNB}$) versus pH plot (Figure 7B). The various pK_a values in different solvent systems are summarized in Table 2 for comparison.

DISCUSSION

Quaternary structure of GST in reverse micelles

Octopus GST is a dimeric protein composed of two identical subunits [6]. The three-dimensional structures of the Alpha-, Mu-, and Pi-class GSTs have been solved by X-ray crystallographic analyses [30–33]. More recently, the detailed structure of squid digestive gland GST was delineated to 2.4 Å resolution [34]. The dimeric interface of the cephalopods' GST is different from that of the vertebrate GST. By amino acid sequence alignment, and gene and three-dimensional structure comparisons with Alpha-, Mu- and Pi-class GSTs, the cephalopods' GST was placed into a separate Sigma class [34,36].

The protein has a roughly globular structure with molecular dimensions of about 6.2 nm × 5.1 nm × 4.6 nm, corresponding to a volume occupied by the dimeric enzyme of approximately 145 nm^3. The inclusive radius of an empty AOT/iso-octane reverse micelle at ω_o 13.88 is 2.48 nm, which corresponds to only 64 nm^3 for the inclusive volume of the reverse micellar vesicles. It seems that at this hydration degree only one subunit of the enzyme molecule is entrapped in each reverse micellar vesicle. It also suggests that only a monolayer of water molecules was bound on the enzyme surface in contact with the polar head group of AOT molecules. However, there are many other factors, including ionic strength, pH, or protein concentration, which influence the actual volume of the vesicle [37]. At low ω_o, the hydrodynamic radii of empty and protein-containing AOT/iso-octane reverse micelles were found to be 2.9 and 4.45 nm

respectively [38]. Direct evidence is thus needed for demonstrating the dissociation of GST in reverse micelles.

According to the theory of Martinek, Kabanov and co-workers [9,11,17], the enzyme activity versus ω_o profile of an oligomeric enzyme will show multiple activity maxima at ω_o values corresponding to the volume of various aggregations of the enzyme molecule. However, the bell-shaped rate versus ω_o plot was also fitted to a theoretical situation in which the enzyme prefers bound water rather than free water [39] and has nothing to do with the dissociation process. We detected only one maximum activity peak at ω_o 13.88. We have checked the pH values of the reverse micellar solution. The pH artifacts could be ruled out [40]. Dissociation of the octopus GST in AOT/iso-octane reverse micelles was demonstrated by cross-linking and SDS/PAGE (Figure 3). Our kinetic data obtained at ω_o 13.88 thus probably represent those for a monomeric GST. If this is the case, then our results indicate that the monomeric GST is enzymically active.

Structural information of the enzyme indicated that the two active centres of GST are structurally independent of each other [30–33]. Results on kinetic studies of GST-α [41,42] and GST-π [43] also suggested two independent active centres of the dimeric GST, but could not demonstrate an enzymically active subunit. On the other hand, using the technique of radiation inactivation, the functionally active unit of GST-μ was demonstrated to be the monomer [44]. Kinetically, co-operativity between subunits was only observed in Cys^{47} mutants [45].

In our case, the kinetic behaviour of octopus GST observed in reverse micelles, whether it is a dimer or a monomer, represents the enzyme properties in a solvent system quite different from that of the aqueous solution. Its implications on the *in vivo* conditions are discussed below.

Kinetic and chemical mechanism of octopus GST in reverse micelles

The results of initial-velocity and product-inhibition studies indicate that the octopus GST conforms to a steady-state random Bi Bi kinetic mechanism instead of a rapid equilibrium one. A similar conclusion was deduced in aqueous solution [7]. The curvature of the double reciprocal plot, as expected for a steady-state random Bi Bi mechanism, was not obvious so the initial-velocity data were fitted to a rapid-equilibrium random Bi Bi model. Fitting the initial-velocity data to eqn. (5) assumes that $K_d = K_m$, thus, $K_{m,GSH}$, $K_{m,CDNB}$ and $K_{d,GSH}$ in Table 2 are all simply dissociation constants and $K_{d,CDNB}$ was obtained from the relationship of $K_{m,GSH} \cdot K_{d,CDNB} = K_{d,GSH} \cdot K_{m,CDNB}$. The relevance of this data treatment has been discussed [7].

The entrapped enzyme showed lower catalytic efficiency compared with that in the aqueous solution. Although formation of reverse micelles was instantaneous, as manifested by the rapid disappearance of turbidity of the solution after mixing, the possibility that some of the GST molecules might first be denatured by exposure to organic solvent or surfactant could not be completely excluded. This may explain the lower catalytic efficiency of GST in reverse micelles. The major kinetic difference is the 36-fold increase in the $K_{m,CDNB}$ value in reverse micelles. The possibility that the enzyme undergoes gross conformational changes in reverse micelles, which hindered the binding with its substrates, does not seem likely because $K_{m,GSH}$ and $K_{d,GSH}$ were hardly affected. A more likely situation is that the hydrophobic substrate CDNB was partitioned between the organic phase and the water pool. The larger $K_{m,CDNB}$ or $K_{d,CDNB}$ was simply due to the smaller concentration of CDNB in the aqueous phase. If the partition coefficient of CDNB between the organic phase and the water phase was considered, the $K_{m,CDNB}'$ value becomes close to that in aqueous solution (Table 1). It can be concluded that the kinetic behaviour of octopus GST in reverse micelles resembles that in aqueous solution, except that the partitioning of the hydrophobic substrate should be considered separately. A theoretical treatment of the kinetic data in reverse micelles for an enzyme involving both polar and apolar substrates was described to include the consideration of the partition coefficient for the apolar substrate [21]. The theory has been tested on 20β-hydroxysteroid dehydrogenase [18]. These discussions, however, only take account of the partition of apolar substrate in an organic solvent and aqueous buffer two-phase system, and do not consider the possibility of partitioning apolar compounds into the surfactant interface, which is experimentally difficult to approach. It is just possible that the data in Figure 4 are explicable as more AOT in the system renders more CDNB in the interface and less CDNB in the aqueous phase, resulting in lower enzyme activity to be detected.

Substantially different results were obtained in the pH studies for the two solvent systems (Figure 7). According to our previous interpretation [7], the molecular pK_a values of 6.56 in Figure 7(A) and 6.70 in Figure 7(B) most likely represent that of the thiol group of bound GSH in the E–GSH–CDNB ternary- and E–GSH binary-complexes respectively. Similar results were obtained in aqueous solution, with slightly larger pK_a values (6.70 and 6.80 respectively). A possible explanation for the discrepancy in pK_a values is that the negative-charged surfactant AOT assists ionization of GSH, hence decreasing the pK_a values [16]. These pK_a values are in accordance with those found in squid GST, which has pK_a values of 6.2 and 6.4 respectively, for the above ternary and binary complexes [34].

The GSH thiolate anion (GS^-) has been demonstrated to be the active GSH species during catalysis and Tyr^7 to be involved in ionization of the enzyme-bound GSH [30–32]. The most attractive candidate for the group with pK_a 8.81 in Figure 7(A) will be Tyr^7 [6], which has to be deprotonated to give a maximum reaction rate. The pK_a value found for Tyr^7 in octopus GST-σ is consistent with the spectroscopically determined value of 8.4 for GST-α [46]. This result is opposite in the two solvent systems. GST may undergo a different reaction mechanism in reverse micelles. The pK_a value of free GSH in reverse micelles was found to be 8.095 ± 0.025 [16]. This is 1.40–1.54 pH unit lower for the bound GSH. The tyrosinate may function as a general base catalyst, facilitating the dissociation of bound GSH and forming a better nucleophile GS^- to attack the *ipso* carbon of CDNB in the nucleophilic aromatic substitution reaction. A similar mechanism has been proposed by Atkins et al. [46]. This mechanism is compatible with the finding of two reactive thiolate species for the GST-μ [47].

Possible physiological significance of the kinetic properties of octopus GST in reverse micelles

The advantage of assaying GST activity in reverse micelles is obvious. The water-insoluble substrate can now be used in much larger concentrations. The strong substrate inhibition by CDNB in reverse micelles was not observed in the aqueous solution due to limited solubility. Whether this phenomenon occurred *in vivo* is an intriguing question. Probably the xenobiotics will never reach a concentration large enough to cause inhibition of GST in viable cells. The failure of fitting CDNB data to eqn. (3) was probably because large concentrations of CDNB caused irreversible enzyme inactivation as demonstrated by Liu et al. [48].

GST is a cytosolic enzyme. It constitutes as much as 10% of the total soluble proteins in the cytoplasm [49]. The finding that GST is sensitive to surfactant (Figure 4) suggests that this

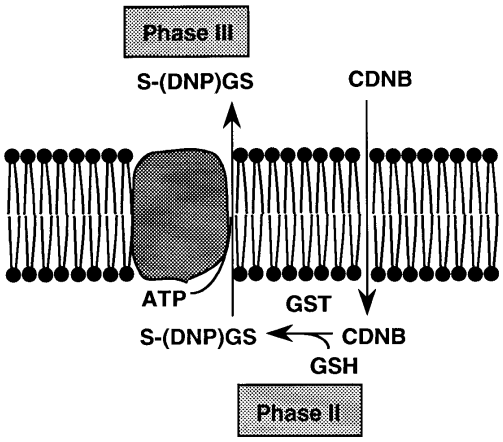

Scheme 1 Schematic model for the elimination of hydrophobic compounds by the cell through the GST and GSH-conjugate pump system

The efficiency of the detoxification mechanism was greatly increased by coupling the phase II conjugation reaction with phase III conjugate pump system due to the affinity of GST with the plasma membrane.

cytosolic enzyme has some affinity with the membranous structure [11,50,51]. Furthermore, the bell-shaped rate versus ω_o plot conforms to a theoretical situation in which the enzyme prefers to be at the interface between the bulk water pool and the hydrocarbon phase [39]. The physiological function of GST is the elimination of xenobiotic hydrophobic compounds. Association of GST with plasma membrane has 2-fold advantages for the cells. First, the toxic effects of xenobiotics to the cell components can be minimized if the conjugation reaction takes place as soon as the xenobiotics get across the membrane barrier. Secondly, the detoxification phase II conjugation process can couple with the phase III conjugate-pump system in a more efficient manner (Scheme 1). If that was the case *in vivo*, then our kinetic results reported in this paper represent the enzyme properties in more physiological conditions.

This work was supported by the National Science Council, Republic of China (NSC 84-2311-B016-001 BA). A preliminary report has been presented at the International Symposium of Biophysics and Structural Biology held in Taipei during May 11–13, 1995. This paper is presented by S.-S.T. in partial fulfillment of a Ph.D. degree (Life Science), National Defence Medical Centre, Taipei.

REFERENCES

1 Mannervik, B. and Danielson, U. H. (1988) CRC Crit. Rev. Biochem. **23**, 283–337
2 Jakoby, W. B. and Ziegler, D. M. (1990) J. Biol. Chem. **265**, 20715–20718
3 Armstrong, R. N. (1991) Chem. Res. Toxicol. **4**, 131–140
4 Rushmore, T. H. and Pickett, C. B. (1993) J. Biol. Chem. **268**, 11475–11478
5 Ishikawa, T. (1992) Trends Biochem. Sci. **17**, 463–468
6 Tang, S. S., Lin, C. C. and Chang, G. G. (1994) J. Protein Chem. **13**, 609–618
7 Tang, S. S. and Chang, G. G. (1995) Biochem. J. **309**, 347–353
8 Luisi, P. L. and Magid, L. J. (1986) CRC Crit. Rev. Biochem. **20**, 409–474
9 Martinek, K., Levashov, A. V., Klyachko, N., Khmelnitski, Y. L. and Berezin, I. V. (1986) Eur. J. Biochem. **155**, 453–468
10 Luisi, P. L., Giomini, M., Pileni, M. P. and Robinson, B. H. (1988) Biochim. Biophys. Acta **947**, 209–246
11 Martinek, K., Klyachko, N. L., Kabanov, A. V., Khmelnitsky, Y. L. and Levashov, A. V. (1989) Biochim. Biophys. Acta **981**, 161–172
12 Luisi, P. L. (1985) Angew. Chem. Int. Ed. Engl. **24**, 439–450
13 Waks, M. (1986) Proteins: Struct. Funct. Genet. **1**, 4–15
14 Luisi, P. L. and Laane, C. (1986) Trends Biotech. **4**, 153–161
15 Chang, G. G., Tsai, L. N., Tang, S. S. and Wang, T. C. (1994) Arch. Biochem. Biophys. **310**, 134–143
16 Tang, S. S. and Chang, G. G. (1995) J. Org. Chem. **60**, 6183–6185
17 Kabanov, A. V., Klyachko, N. L., Nametkin, S. N., Merker, S., Zaroza, A. V., Bunik, V. I., Ivanov, M. V. and Levashov, A. V. (1991) Protein Eng. **4**, 1009–1017
18 Tyrakowska, B., Verhaert, R. M. D., Hilhorst, R. and Veeger, C. (1990) Eur. J. Biochem. **187**, 81–88
19 Bradford, M. M. (1976) Anal. Biochem. **72**, 248–254
20 Matzke, S. F., Creagh, A. L., Haynes, C. A., Prausnitz, J. M. and Blanch, H. W. (1991) Biotechnol. Bioeng. **40**, 91–102
21 Verhaert, R. M. D., Hilhorst, R., Vemuë, M., Schaafsma, T. J. and Veeger, C. (1990) Eur. J. Biochem. **187**, 59–72
22 Pabst, M. J., Habig, W. H. and Jakoby, W. B. (1974) J. Biol. Chem. **249**, 7140–7150
23 Laane, C., Hilhorst, R. and Veeger, C. (1987) Methods Enzymol. **136**, 216–227
24 Chang, G. G., Huang, T. M., Huang, S. M. and Chou, W. Y. (1994) Eur. J. Biochem. **225**, 1021–1027
25 Huang, T. M. and Chang, G. G. (1992) Biochemistry **31**, 12658–12664
26 Luisi, P. L. and Steinmann-Hofmann, B. (1987) Methods Enzymol. **136**, 188–216
27 Perrella, F. W. (1988) Anal. Biochem. **174**, 437–447
28 Chang, G. G. and Shiao, S. L. (1994) Eur. J. Biochem. **220**, 861–870
29 Segel, I. H. (1975) Enzyme Kinetics, pp. 907–913, John Wiley & Sons, New York
30 Dirr, H., Reinemer, P. and Huber, R. (1994) Eur. J. Biochem. **220**, 645–661
31 Sinning, I., Kleywegt, G. J., Cowan, S. W., Reinemer, P., Dirr, H. W., Huber, R., Gilliland, G. L., Armstrong, R. N., Ji, X., Board, P. G., Olin, B., Mannervik, B. and Jones, T. A. (1993) J. Mol. Biol. **232**, 192–212
32 Armstrong, R. N. (1994) Adv. Enzymol. Relat. Areas Mol. Biol. **69**, 1–44
33 García-Sáez, I., Párraga, A., Phillips, M. F., Mantle, T. J. and Coll, M. (1994) J. Mol. Biol. **237**, 298–314
34 Ji, X., von Rosenvinge, E. C., Johnson, W. W., Tomarev, S. I., Piatigorsky, J., Armstrong, R. N. and Gilliland, G. L. (1995) Biochemistry **34**, 5317–5328
35 Fletcher, P. D. I., Howe, A. M. and Robinson, B. H. (1987) J. Chem. Soc., Faraday Trans. I, **83**, 985–1006
36 Buetler, T. M. and Eaton, D. L. (1992) Environ. Carcinogen. Ecotoxicol. Rev. **C10**, 181–203
37 Rahaman, R. S. and Hatton, T. A. (1991) J. Phys. Chem. **95**, 1799–1811
38 Chatenay, D., Urbach, W., Nicot, C., Vacher, M. and Waks, M. (1987) J. Phys. Chem. **91**, 2198–2201
39 Bru, R., Sánchez-Ferrer, A. and Garcia-Carmona, F. (1989) Biochem. J. **259**, 355–361
40 Walde, P., Mao, Q., Bru, R., Luisi, P. L. and Kuboi, R. (1992) Pure Appl. Chem. **64**, 1771–1775
41 Danielson, U. H. and Mannervik, B. (1985) Biochem. J. **231**, 263–267
42 Aceto, A., Caccuri, A. M., Sacchetta, P., Bucciarelli, T., Dragani, B., Rosato, N., Federici, G. and Di Ilio, C. (1992) Biochem. J. **285**, 241–245
43 Dirr, H. W. and Reinemer, P. (1991) Biochem. Biophys. Res. Commun. **180**, 294–300
44 Boyer, T. D. and Kempner, E. S. (1992) Anal. Biochem. **207**, 51–57
45 Ricci, G., Bello, M. L., Caccuri, A. M., Pastore, A., Nuccetelli, M., Parker, M. W. and Federici, G. (1995) J. Biol. Chem. **270**, 1243–1248
46 Atkins, W. M., Wang, R. W., Bird, A. W., Newton, D. J. and Lu, A. Y. H. (1993) J. Biol. Chem. **268**, 19188–19191
47 Graminski, G. F., Zhang, P., Sesay, M. A., Ammon, H. L. and Armstrong, R. N. (1989) Biochemistry **28**, 6252–6258
48 Liu, L.-F., Hong, J.-L., Tsai, S.-P., Hsieh, J.-C. and Tam, M.-F. (1993) Biochem. J. **296**, 189–197
49 Jakoby, W. B. (1987) in Enzyme Mechanism (Page, H. I. and Williams, A., eds.), pp. 468–476, Royal Society of Chemistry, Cambridge, U.K.
50 Kabanov, A. V., Levashov, A. V., Klyachko, N. L., Namyotkin, S. N. and Pshezhetsky, A. V. (1988) J. Theor. Biol. **133**, 327–343
51 Levashov, A. V., Rariy, R. V., Martinek, K. and Klyachko, N. L. (1993) FEBS Lett. **336**, 385–388

Received 12 June 1995/12 October 1995; accepted 12 December 1995